FAST TRACK COMMUNICATION

Graphene based quantum dots

H G Zhang[1], H Hu[1], Y Pan[1], J H Mao[1], M Gao[1], H M Guo[1], S X Du[1], T Greber[2] and H-J Gao[1]

[1] Institute of Physics, Chinese Academy of Sciences, PO Box 603, Beijing 100190, People's Republic of China
[2] Physik-Institut, University of Zürich, Winterthurerstrasse 190, CH-8057 Zürich, Switzerland

E-mail: greber@physik.uzh.ch and hjgao@iphy.ac.cn

Abstract
Laterally localized electronic states are identified on a single layer of graphene on ruthenium by low temperature scanning tunneling spectroscopy (STS). The individual states are separated by 3 nm and comprise regions of about 90 carbon atoms. This constitutes a highly regular quantum dot-array with molecular precision. It is evidenced by quantum well resonances (QWRs) with energies that relate to the corrugation of the graphene layer. The dI/dV conductance spectra are modeled by a layer height dependent potential-well with a delta-function potential that describes the barrier for electron penetration into graphene. The resulting QWRs are strongest and lowest in energy on the isolated 'hill' regions with a diameter of 2 nm, where the graphene is decoupled from the surface.

(Some figures in this article are in colour only in the electronic version)

1. Introduction

The exfoliation of graphene [1] rapidly raised remarkable interest in the fields of material science and condensed-matter physics [2–10]. The low conduction electron density paired with a large electron mobility [5] allows the construction of p–n junctions [6] and transistors [7]. Novel electronic properties are expected if the dimensionality of the graphene is tuned. For example, graphene nanoribbons (1D) are semiconducting [8]. For zero-dimensional (0D) graphene, i.e. small graphene flakes or polycyclic aromatic hydrocarbons [9–11], non-dispersing, localized electronic states with a gap that decreases with the number of carbon rings are anticipated. However, not much is known about the transition from a localized, dot like hexagonal carbon network to a delocalized one, also because it is difficult to prepare 'zero-dimensional' graphene. Previous studies showed that the honeycomb symmetry of graphene can be broken by substrates, leading to the formation of energy gaps [12, 13], similar to the case of hexagonal boron nitride layers, where the gap is due to the differences between boron and nitrogen atoms [14]. It turns out that the concerted use of substrates is one attractive route towards the construction of 0D graphene structures with the potential to open up

new opportunities in optoelectronics, nano-electronics, and for single electron devices.

In this fast track communication, we report on the observation and identification of 'zero-dimensional' graphene based quantum dots in the graphene/Ru(0001) system, denoted as g/Ru(0001). They emerge in a self-assembly process on a corrugated 3 nm super-lattice and exhibit laterally and vertically confined states that relate to the corrugation of the surface. The states show up as sharp resonances in the conductance spectra in scanning tunneling spectroscopy (STS) with energies that correspond to the eigenvalues of a model potential describing graphene/Ru junctions with different layer heights. An extra resonance above the vacuum level is caused by the graphene and we call it quantum well resonance (QWR). As was found for quantum well states in lead films [15], its energy is modulated on the nanometer scale, though here the corrugation of the single layer induces a much stronger effect.

2. Results and discussion

The experiments were performed in an Omicron low temperature scanning tunneling microscopy (STM) system with a base pressure of 10^{-10} mbar. The method to clean
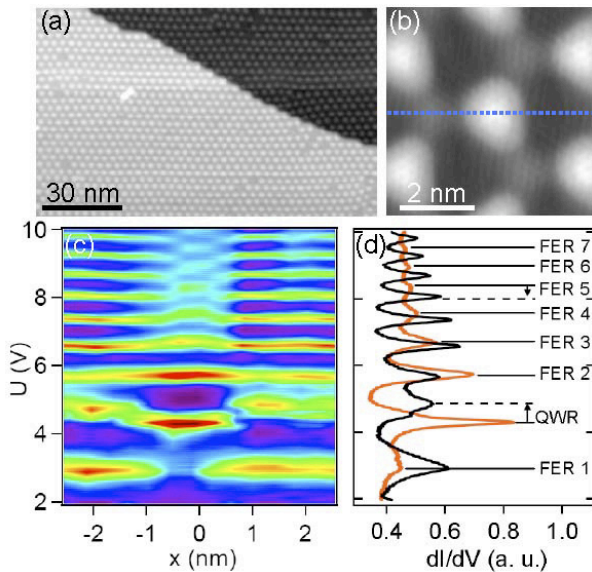
Figure 1. STM image and STS for monolayer graphene on Ru(0001). (a) Large-scale ($U_t = -2.0$ V, $I_t = 100$ pA) STM topographic image across two substrate terraces separated by a monoatomic step. (b) A high resolution image, the dotted line indicates the cut shown in (c). (c) Color-scale map of the conductance (dI/dV) into the unoccupied substrate states as a function of tunneling voltage U and position along the dashed line marked in (b). The center of the hill is taken as the zero position. (d) Conductance dI/dV spectra on the hill $x = -0.2$ nm (orange, grey) and the valley $x = 2.0$ nm (black). The spectra are taken at constant current $I_t = 100$ pA.

the substrate and fabricate the graphene has been described elsewhere [16]. Distance–voltage (z–V) spectroscopy and corresponding dI/dV conductance spectra were acquired with engaged loop gain using a lock-in technique with a 10 mV$_{rms}$ sinusoidal modulation signal at 793 Hz, which is superposed to the bias voltage U. Positive bias voltages correspond to tunneling of electrons from the tip to unoccupied states in the sample.

Figure 1 displays high resolution STM and STS data from g/Ru(0001) recorded at 4.5 K. In figure 1(a) a large-scale image of the superstructure with protrusions separated by 3 nm is shown. The perfectly ordered single layer graphene spans across two terraces separated by an atomic step. Figure 1(b) is a high resolution zoom in with atomic resolution. The protrusions or 'hills' with triangular shape emerge with a diameter of 2 nm or about 90 carbon atoms and are separated by 'valleys'. The 3.11 nm periodicity is induced by the lattice mismatch of about 10% between the substrate and the graphene [17]. The height of the protrusions is between 0.1 and 0.15 nm as measured with STM [16, 18, 19] or found from density functional theory calculations [20], and affects the properties of the structure dramatically.

It has been shown that the hills have a 0.25 eV higher local work function compared to the 'valley' regions, where the graphene sheet is closely bound to the substrate [14]. A splitting in the C 1's core level photoemission spectrum confirmed two species of 'graphene' on g/Ru(0001) that were

related to the corrugation, where about one third has a 0.6 eV lower binding energy [21]. On the other hand, in the valence bands no such splitting could be found. Only one dispersing π band with a relatively large gap was observed [14]. This seeming paradox of absence of a corrugation induced splitting in the valence band [22] may be resolved if we assign to the hills a molecule like behavior as isolated quantum dots, without dispersion. The isolation of these dots and the concomitant electronic states are related to the corrugation of the structure, where the lift off of the hills causes lateral localization. The vertical localization arises from the interface and is pronounced by the decoupling of the graphene layer from the substrate.

dI/dV conductance spectra are shown as a U versus x map in figure 1(c), where U is the tunneling voltage and the x axis corresponds to the dotted line in figure 1(b). The color code represents the conductance from the tip into unoccupied states of g/Ru(0001). Clearly, a series of resonances at distinct tunneling voltages is observed. The energies and the sharpness of the resonances change within the 5 nm cut across the super-cell. One of these peaks, the second lowest one, shows a behavior that deviates from the others, which are the well known field emission resonances (FERs), sometimes called image potential states, ubiquitous at tip–surface junctions [23, 24]. The FER energies may be used to determine the local work function, whereby a decrease in energy indicates a decrease of the work function of the probed surface region [25, 26]. For the present case, g/Ru(0001), the FER energy increase on the hill confirms the local work function shift as found by photoemission from adsorbed xenon [14]. The peak that opposes the trend of the FERs is, as it is shown here, a quantum well resonance (QWR), which indicates the quantum dot nature of the hills. It can be seen that this resonance undergoes, within less than 1 nm, an abrupt decrease in energy (0.5 eV) in going from the valley to the hill of the superstructure. Intuitively, like for a particle in a box, this decrease in energy reflects the increase of vertical delocalization with height. Therefore, the hills act like 'mesas', displaying an isolated nanoscopic electronic system. Figure 1(d) shows two spectra, one on a hill and one in a valley, at positions $x = -0.2$ and 2.0 nm. The QWR on the hills displays a sharp peak with a high Q-factor.

In the following we substantiate the physical picture leading to the interpretation of the hills as quantum dots, and explain the opposite trends between the FERs and the QWR. Figure 2 shows a one-dimensional model of the potential for the tip/g/Ru(0001) junction with positive bias voltages and the concomitant solutions of the one-dimensional Schrödinger equation. In figure 2(a) the potential in the valley and in figure 2(b) that on the hills are depicted. The potential in the vacuum is modeled as the work function plus an image potential $U(z)$ proportional to $1/4(z - z_i)$, with z_i being the position of the image potential plane, plus a linear term that mimics the potential gradient between the tip and the sample. The relative z-position of the tip is measured, and thus up to the offset z_o, not a fit parameter. The essential ingredient of the model, the interface between the graphene and the vacuum, is described with a delta-function potential centered on the image plane $\gamma\delta(z - z_i)$. Such a barrier has been used by Kubby,
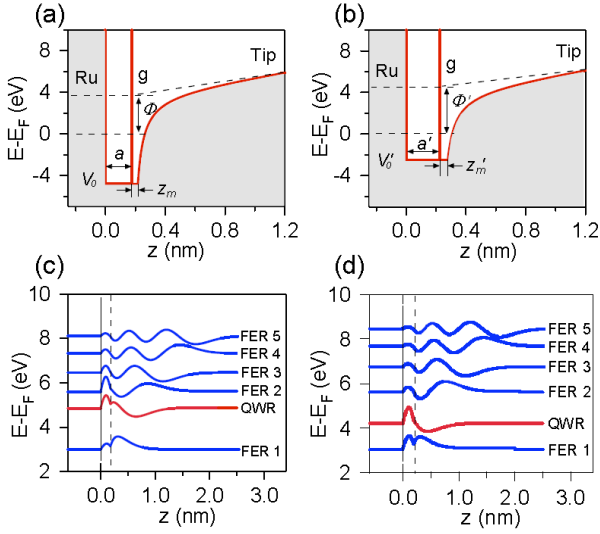
Figure 2. One-dimensional potential models for the QWR and the FERs on g/Ru(0001), (a) for the valley (b) for the hill. The vertical red lines indicate the delta-function potentials. See parameters in table 1. The corresponding energies E_n and amplitudes of the normalized wavefunctions Ψ_n are displayed in (c) and (d). The dashed lines indicate the positions of the delta-function potentials.

Table 1. Parameters obtained from the fit of the model in figure 2 to the observed resonances. For the valley $a + z_m$ was set close to the literature value of the graphene distance above the Ru substrate of 0.22 nm [20], V_o, z_o and γ are left as free parameters. z_o corresponds to the effective tip–sample distance at $U = 2.0$ V and $I = 0.1$ nA in the valley. On the hill z_o' is set to the fit value from the valley, V_o' and γ' are left as free parameters. For $a'-a$, a value of 50 pm has been assumed. The local work functions Φ and Φ' for both regions are taken from the experiment [14].

	a (nm)	V_o (eV)	γ (eV Å^{-1})	z_o (nm)	z_m (nm)	Φ (eV)
Valley	0.175	−4.8	34	1.55	0.041	3.9
Hill	0.225	−2.5	30	1.55	0.053	4.2

Wang and Greene for the description of tunneling spectra in Sn/Si heterojunctions [27]. It accounts for the transmission and reflectivity of low energy electrons approaching graphene along z [28, 29] and gives rise to the distinction between QWR and FER (see below). The graphene is a rectangular quantum well with a width a and a', and a depth V_o and V_o' for valley and hill, respectively. The substrate is a perfect hard wall mirror, which is justified with the large gap in the relevant energy window along $\bar{\Gamma}$ [30]. This potential model is solved numerically by the Numerov algorithm [31], and the parameters from the fit are shown in table 1.

The model reproduces the observed experimental trends of the conductance peak energies, i.e. the upward shift of the FERs and the downward shift of the QWR in going from the valley to the hill. The smaller potential V_o' on the hills compared to V_o in the valleys is taken as an indication of a different bonding of the graphene to the Ru. Of course, the well potential of the real system is more complex than that of the one-dimensional model. In particular the model does not account for the lateral localization. For an electron in a cylinder
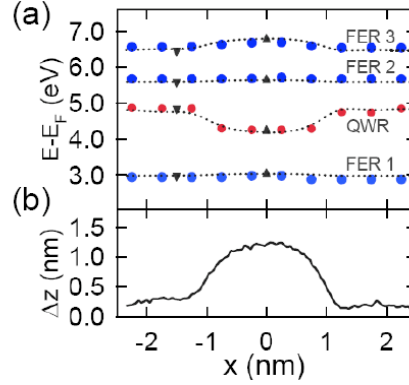

Figure 3. (a) Experimental (circles) and theoretical (triangles) resonance energies of the first three FER$_n$ ($n = 1, 2, 3$) and the QWR as a function of the positions across the super-cell. The dashed lines are obtained by interpolating the theoretical results (solid triangles) linearly using the line profile in (b). (b) The line profile ($U_t = -2.0$ V) shows the apparent height across the hill region of the graphene superstructure.

with a radius of 1.0 nm we expect an additional localization energy of 0.2 eV, which is implicitly considered via the value of V_o'.

The 1D model delivers in a clear way the wavefunctions and thus allows the distinction of QWR and FERs by their locations. In figures 2(c) and (d) the amplitudes of the wavefunctions are plotted along z. The FERs are mainly localized in the vacuum/graphene interface and the QWRs are localized in the graphene/ruthenium well. These states are the solutions of the 1D Schrödinger problem, with energies E_n and wavefunctions Ψ_n, where n denotes the number of nodes in $(0, +\infty)$. Since one of the potential walls is penetrable, the QWR will hybridize with any FER with similar energy. This hybridization also implies that the FERs close to QWRs have amplitude in the well, and vice versa, the QWR gains amplitude outside the well, which is expected to have an effect on the dI/dV spectra. The distinction between FER and QWR is not sharp, though it singles out the peculiar role of the QWR and identifies the quantum dots on g/Ru(0001).

In figure 3(a) the experimentally observed resonances on the quantum dots are compared to the model calculations. The intermediate energies between the valley and hill situation are interpolated linearly with the height as measured with STM (figure 3(b)). The agreement is excellent and confirms the validity of the model.

The concept of QWR as we apply it, has also been used in the framework of rare gas layers [32]. It recalls the situation in a Fabry–Perot interferometer [33], or a resonance cavity, where the delta-function potential of the vacuum/graphene interface acts as a semi-transparent mirror and the Ru substrate as a perfect mirror. Although the physical picture is reminiscent to the so called transmission resonances [27], we believe the term quantum well resonance to be more appropriate. The electrons collect phase in a multiple scattering process [34] bouncing in the graphene layer. This is different from the single scattering process encountered in a transmission resonance [35], which
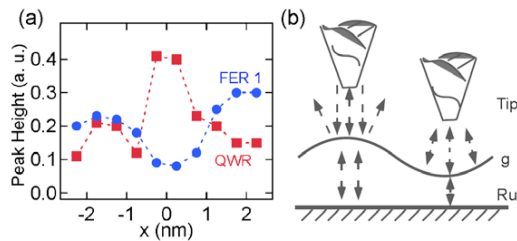
Figure 4. (a) Conductance maxima of the FER$_1$ and QWR as functions of position across the g/Ru(0001) super-cell. On the hills the conductance into the QWR is maximum, while the FER almost vanishes. (b) Schematic illustration of the tip–sample geometry that affects the intensities of the two differently located states in opposite ways.

is broader in energy than a multiple scattering resonance. It is not clear to which extent it is related to the unoccupied state on graphite, 3.6 eV above the Fermi energy that does not disperse along z [36]. Though, the currently reported state should not be mixed up with the quantized oscillations in the reflectivity of low energy electrons from thin graphite layers on SiC [28]. Also we would like to add that the QWRs in the present situation may not be described with a double Rydberg series, as is expected for free standing graphene [37, 38].

The main statement of this paper is the observation of an isolated electronic resonance state, localized on 2 nm graphene hills. This quantum dot picture is further substantiated in figure 4. FER$_1$ on the hills is much weaker compared to the valleys. This is likely to have an electrostatic explanation, indicating the importance of the lateral dimensions: on the hills the electrostatic potential is convex in shape due to the higher local work function that defocuses the electrons out of the resonator cavity, while they are focused into the resonator cavity in the concave potential of the valleys. This also offers an explanation for the observations of lateral FER strength modulations on certain NaCl islands on Ag(001), where the FERs are stronger as well on top of low work function patches [39]. On the other hand, the QWR on the hill is strongest. Since the electrons in the QWR are mainly localized in the graphene, the above defocusing argument does not apply, but the decoupling of the graphene from the substrate increases the resonance lifetime (also see figure 1(d)). This explanation of the resonance strength is illustrated in figure 4(b) where the influence of the topography and the electrostatic landscape is sketched for the tip/g/Ru(0001) tunneling junction.

3. Conclusions

In summary, the formation of graphene based quantum dots on Ru(0001) made from about 90 carbon atoms is evidenced by means of scanning tunneling spectroscopy. The local tunneling conductance peaks at distinct tunneling voltages are explained with a quantum well resonance and field emission resonances. The QWR on the hills of the corrugated graphene is very strong and has a distinctly lower energy ($\approx$500 meV) compared to that in the valleys. Our observations demonstrate that graphene on ruthenium constitutes an ordered array of quantum dots, with

both lateral and vertical confinement. The structures are small enough that they are candidates for single electron physics at room temperature and they bridge zero-dimensional molecule like and two-dimensional graphene. The quantum dots may e.g be manipulated by magnetic fields or the adsorption of molecules or the choice of other substrates. We expect that this structure is just the first example of periodic graphene based quantum dot systems and the material has significant potential for new applications in single electron quantum devices.

References

[1] Novoselov K S *et al* 2004 *Science* **306** 666
[2] Novoselov K S *et al* 2005 *Nature* **438** 197
[3] Novoselov K S *et al* 2007 *Science* **315** 1379
[4] Bolotin K I *et al* 2009 *Nature* **462** 196
[5] Morozov S V *et al* 2008 *Phys. Rev. Lett.* **100** 016602
[6] Williams J R *et al* 2007 *Science* **317** 638
[7] Sordan R *et al* 2009 *Appl. Phys. Lett.* **94** 073305
[8] Li X *et al* 2008 *Science* **319** 1229
[9] Ponomarenko L A *et al* 2008 *Science* **320** 356
[10] Müller M *et al* 1998 *Chem. Eur. J.* **4** 2099
[11] Sols F, Guinea F and Castro Neto A H 2007 *Phys. Rev. Lett.* **99** 166803
[12] Zhou S Y *et al* 2007 *Nat. Mater.* **6** 770
[13] Giovannetti G *et al* 2008 *Phys. Rev. Lett.* **101** 026803
[14] Brugger T *et al* 2009 *Phys. Rev.* B **79** 045407
[15] Altfelder I B *et al* 2002 *Phys. Rev. Lett.* **88** 206801
[16] Pan Y *et al* 2009 *Adv. Mater.* **21** 2777
[17] Martoccia D *et al* 2008 *Phys. Rev. Lett.* **101** 126102
[18] Marchini S, Günther S and Wintterlin J 2007 *Phys. Rev.* B **76** 075429
[19] V'azquez de Parga A L *et al* 2008 *Phys. Rev. Lett.* **100** 056807
[20] Wang B *et al* 2008 *Phys. Chem. Chem. Phys.* **10** 3530
[21] Preobrajenski A B *et al* 2008 *Phys. Rev.* B **78** 073401
[22] Corso M *et al* 2004 *Science* **303** 217
[23] Becker R S *et al* 1985 *Phys. Rev. Lett.* **55** 987
[24] Binnig G *et al* 1985 *Phys. Rev. Lett.* **55** 991
[25] Ploigt H-C *et al* 2007 *Phys. Rev.* B **76** 195404
[26] Ruffieux P *et al* 2009 *Phys. Rev. Lett.* **102** 086807
[27] Kubby J A, Wang Y R and Greene W J 1990 *Phys. Rev. Lett.* **65** 2165
[28] Hibino H *et al* 2008 *Phys. Rev.* B **77** 075413
[29] Sutter P W, Flege J-I and Sutter E A 2008 *Nat. Mater.* **7** 406
[30] Pelzer T *et al* 2000 *J. Phys.: Condens. Matter* **12** 2193
[31] Dunn D *et al* 1989 *J. Phys. A: Math. Gen.* **22** L1093
[32] Marinica D C *et al* 2003 *Surf. Sci.* **504** 457
[33] Tringides M C, Jalochowski M and Bauer E 2007 *Phys. Today* **60** 50
[34] Smith N V *et al* 1994 *Phys. Rev.* B **49** 332
[35] Su W B *et al* 2006 *J. Phys.: Condens. Matter* **18** 6299
[36] Fauster Th *et al* 1983 *Phys. Rev. Lett.* **51** 430
[37] Silkin V M *et al* 2009 *Phys. Rev.* B **80** 121408
[38] Bose S *et al* 2010 *New J. Phys.* **12** 023028
[39] Pivetta M *et al* 2005 *Phys. Rev.* B **72** 115404
[40] Zhang H G *et al* 2009 arXiv:0911.4024